Published in final edited form as:

Oncogene. 2009 August 27; 28(34): 3022–3032. doi:10.1038/onc.2009.165.

BMI1 Cooperates with H-RAS to Induce an Aggressive Breast Cancer Phenotype with Brain Metastases

Mark J. Hoenerhoff[1], **Isabel Chu**[1], **Dalit Barkan**[1], **Zi-yao Liu**[1], **Sonal Datta**[2], **Goberdhan P. Dimri**[2], and **Jeffery E. Green**[1]

[1]Transgenic Oncogenesis Group, Laboratory of Cancer Biology and Genetics, National Cancer Institute, National Institutes of Health, Bethesda, Maryland, USA

[2]Division of Cancer Biology and Department of Medicine, NorthShore University HealthSystem Research Institute, Feinberg School of Medicine, Northwestern University, Evanston, Illinois, USA

Abstract

BMI1 is a member of the polycomb group of transcription repressors that functions in stem cell maintenance and oncogenesis through inhibition of the *INK4A/ARF* tumour suppressor locus. Overexpression of BMI1 is associated with poor prognosis in several human cancers, including breast cancer. We have previously shown that BMI1 collaborates with H-RAS to induce transformation of MCF10A human mammary epithelial cells via dysregulation of multiple growth pathways independent of the *INK4A/ARF* locus. In this study, we demonstrate that BMI1 collaborates with H-RAS to promote increased proliferation, invasion, and resistance to apoptosis in vitro, and an increased rate of spontaneous metastases from mammary fat pad xenografts including novel metastases to the brain. Furthermore, in collaboration with H-RAS, BMI1 induced fulminant metastatic disease in the lung using a tail vein model of haematogenous spread through accelerated cellular proliferation and inhibition of apoptosis. Finally, we show that knockdown of BMI1 in several established breast cancer cell lines leads to decreased oncogenic behaviour in vitro and in vivo. In summary, BMI1 collaborates with H-RAS to induce an aggressive and metastatic phenotype with the unusual occurrence of brain metastasis, making it an important target for diagnosis and treatment of aggressive breast cancer.

Keywords

BMI1; H-RAS; breast cancer; metastasis

INTRODUCTION

Although metastasis remains the major cause of mortality in breast cancer patients (Vernon *et al.*, 2007), mechanisms of metastatic progression and disease recurrence remain poorly

Corresponding author: Jeffery E. Green, MD, Head, Transgenic Oncogenesis Group, Laboratory of Cancer Biology and Genetics, National Cancer Institute, National Institutes of Health, 37 Convent Drive, Building 37, Room 4054, Bethesda, MD, USA, Phone: (301) 435-5193, Email: jegreen@nih.gov.

understood. Significant improvements have been made in identifying patients at earlier stages of disease, but even patients with minimal disease at initial diagnosis have up to a 30% risk of recurrence many years after the apparently successful treatment of the primary disease (Brackstone *et al.*, 2007; Fisher *et al.*, 2001; Wallgren *et al.*, 2003). Thus, it is critical that identifying underlying molecular mechanisms regulating metastatic processes in breast cancer be elucidated.

B lymphoma Moloney murine leukaemia virus insertion region-1 (BMI1), a member of the polycomb group (PcG) of transcription repressors, was first identified as a Myc-cooperating oncogene in murine B and T-cell lymphomas (Dimri *et al.*, 2002; Haupt *et al.*, 1991; Haupt *et al.*, 1993; Jacobs *et al.*, 1999). Several recent studies have suggested a link between BMI1 expression, mammary carcinogenesis (Dimri *et al.*, 2002; Lessard and Sauvageau, 2003), and regional lymph node metastasis in invasive ductal breast carcinoma (Kim *et al.*, 2004). Additionally, BMI1 has recently been associated with a stem cell-like 11 gene expression microarray signature predictive of a short interval to disease recurrence following therapy, increased likelihood of metastatic disease, and poor response to therapy in multiple types of human cancer, including prostate, lung, ovarian, urinary bladder, lymphoma, mesothelioma, medulloblastoma, glioma, acute myeloid leukaemia, and breast cancer (Glinsky *et al.*, 2005).

We have recently shown that BMI1 collaborates with H-RAS to transform MCF10A human mammary epithelial cells through dysregulation of multiple growth pathways via *INK4A-ARF*-independent mechanisms, including the ERK/MAPK and AKT pathways, and induces poorly differentiated and locally aggressive tumours in severe combined immunodeficient (SCID) mouse xenograft models (Datta *et al.*, 2007). In this study, we examined the effects of BMI1 expression on enhancing the aggressive properties of tumour cells, including metastasis. We demonstrate that overexpression of BMI1 in MCF10A cells overexpressing H-RAS results in a marked spindle-type change in cell morphology, increased proliferation, increased invasive properties, and a markedly decreased apoptotic response to DNA damage. Importantly, the overexpression of BMI1 in MCF10A+H-RAS cells significantly increases spontaneous metastatic disease in mice with the extremely unusual dissemination of metastases to the brain. Similarly, tail vein cell injection of BMI1 and H-RAS overexpressing cells leads to rapid and fulminant metastatic lung disease, which is not observed with cells over-expressing H-RAS alone. Consistent with these observations, knocking down expression of BMI1 with shRNA in several human breast cancer cell lines significantly reduces proliferation and invasion, increases susceptibility to DNA damage-induced apoptosis, and delays tumour onset in xenograft models. These results provide functional evidence that BMI1 can cooperate with H-RAS to dramatically increase the aggressive and metastatic properties of tumours, and suggests that BMI1 may be an important target in tumours that overexpress this gene.

MATERIALS AND METHODS

Cell lines, vectors, and plasmids

Culture of MCF10A, MCF10A+BMI1, MCF10A+H-RAS, and MCF10A+H-RAS+BMI1 cells have been previously described (Datta *et al.*, 2007). MDA-MB-231 and MCF7 cells were grown in DMEM high glucose 1× (Gibco) supplemented with 10% fetal bovine serum

(FBS) (Gibco), and penicillin/streptomycin (Gibco). ZR75-1 cells were grown in RPMI 1640 with 2 mM L-glutamine (Gibco) supplemented with 10% FBS (Gibco), penicillin/streptomycin (Gibco), sodium bicarbonate (1.5 g/L, Gibco), glucose (4.5 g/L, Sigma), HEPES (10 mM, Gibco), and sodium pyruvate (1 mM, Gibco). Retroviruses expressing BMI1 and H-RAS were produced and transduced into MCF10A cells as described (Dimri *et al.*, 2002). Lentivirus containing GFP (pSico) was used to trasduce MCF10A+H-RAS and MCF10A+H-RAS+BMI1 cells by standard protocol (Promega, Madison WI). MDA-MB-231, MCF7, ZR75-1, and MCF10A+H-RAS+BMI1 cells were transduced with BMI1 shRNA lentiviral vector (LV-pLL3.7+BMI1-i) and empty shRNA lentiviral vector (LV-pLL3.7), both expressing green fluorescent protein (GFP), kindly provided by Max Wicha (Liu *et al.*, 2006). See Supplementary Methods for further details.

Cell proliferation, apoptosis, and invasion assays—Cell proliferation assays were performed using the Cell Titer 96® Aqueous MTS-formazan proliferation assay (Promega, Madison WI). This assay measures the bioreduction of MTS tetrazolium by cells to a coloured formazan dye that is soluble in culture medium and is directly proportional to the number of living cells. Cells were cultured in a 96-well plate at 1×10^3 cells per well (with eight repeats), and growth curves were established by measuring the absorbance at 490 nm at 24 hr time intervals following the addition of 20μl of MTS reagent. Apoptosis assays were performed using the Cell Death Detection ELISA^{PLUS} sandwich ELISA (Roche, Indianapolis IN) to detect histone-complexed DNA fragments (mono- and oligonucleosomes) out of the cytoplasm of cells undergoing apoptosis. Cells were cultured in a 96 well plate at 1×10^3 cells per well (with eight repeats) for 24 hours. Apoptosis was measured following treatment of each cell line with 100 mM etoposide after 12 and 24 hr for MCF10A-derived cell lines, and after 48 hr for shRNA expressing or vector control cell lines. Invasion assays were performed using the BD Matrigel invasion chamber assay (BD Bioscences, Bedford MA) for BMI1 overexpression experiments (with four repeats), or the CytoSelect™ 24-well format (with four repeats). This assay measures the ability of cells to invade through a Matrigel matrix overlying a membrane containing 8μm pores. The Matrigel matrix recapitulates the extracellular matrix in vitro, and occludes the membrane pores, preventing non-invasive cells from traveling across the membrane towards a serum chemoattractant. Invasive cells are able to invade through the Matrigel matrix and through the pores along the serum gradient, and thus the number of cells on the opposite side of the membrane serves as a measurement of invasion. To determine the effects of BMI1 expression on the expression of proteins regulating the DNA damage checkpoint and apoptosis pathways, MCF10A-derived cells were treated for 48hr with 100um etoposide (Sigma, St. Louis, MO) and processed for Western blot analyses. See Supplementary Methods for additional details.

Western blot analysis

Western blots were performed using standard assays as previously described (Datta *et al.*, 2007). See Supplementary Methods for additional details.

Animals, necropsy, and histopathology—Cohorts of 10 six-week-old female SCID mice (NCI Frederick, MD) were injected in the right axillary mammary fat pad with 1×10^6

cells. Tumour growth was measured weekly by calliper. Additional cohorts of 10 six-week-old female mice were injected with 1×10^6 cells via the tail vein. Mice were followed for six weeks. Mice were euthanized once tumours reached 2 cm in diameter, or when mice became clinically ill. All animal work was performed following NIH guidelines under an approved animal protocol. Following euthanasia of mice that had received intramammary fat pad cell injections, tumour, brain, lung, heart, liver, spleen and kidney were collected, and either frozen in OCT freezing medium or fixed in 4% paraformaldehyde (PFA), processed into paraffin blocks, sectioned at 4 μm, and stained with haematoxylin and eosin (H&E). Pieces of tumours were snap frozen in liquid nitrogen for further protein and RNA analysis. Selected areas were photographed using an Olympus DP70 (Olympus) digital camera.

Ex vivo imaging experiments: GFP-labelled MCF10A-H-RAS and MCF10A-BMI1+H-RAS cells were sorted by Fluorescence Activated Cell Sorting (FACS) for high GFP expression. Two cohorts of 15 six-week-old female mice each were used, and each cohort received 1×10^6 MCF10A-H-RAS+GFP or MCF10A-BMI1+H-RAS+GFP cells via tail-vein injection. Mice were euthanized at two hours (n=2), two days (n=5), one week (n=5), and four weeks (n=3) after injection. Lungs were harvested at the time of necropsy, infused with 1 ml of 1× PBS, and visualized under a fluorescent microscope to detect GFP-labelled cells (Zeiss, Thornwood NY). GFP signal was measured at 4× magnification and quantified using ImagePro image analysis software (Media Cybernetics, Bethesda MD) examining at least ten fields per animal, and expressed as average pixels per field.

Immunohistochemistry and TUNEL assay: Paraffin-embedded and frozen sections of primary tumours and lungs with metastatic lesions were stained using a rabbit polyclonal antibody for Ki67 (Vector Laboratories) or by TUNEL for apoptosis (Chemicon, Temecula CA) as described in the Supplementary Methods. Ki67 and Apoptag staining was assessed at 10× magnification evaluating at least ten fields per specimen (n=3), and signal was quantified either as labelled cells per field, or by using ImagePro image analysis software (Media Cybernetics, Bethesda MD) as labelled pixels per field.

Statistical Analyses—Proliferation, apoptosis, and invasion assays for MCF10A-derived cell lines were analyzed using one-way ANOVA with Tukey's post-test. Proliferation, apoptosis, and invasion assays using shRNA-induced cell lines were analyzed with a Student's T-test (GraphPad Prism 4.02 [La Jolla CA] was used for all statistical analyses). GFP immunofluoresence, Ki67 immunolabeling, and TUNEL staining in intravenous xenografts were analyzed using a Student's T-test. Subcutaneous xenograft tumour data from MCF10A-derived and shRNA-induced tumours were analyzed with a Two-way ANOVA with Bonferroni correction.

RESULTS

BMI1 and H-RAS collaborate to alter the morphologic phenotype of MCF10A human mammary epithelial cells in 3D culture

We previously demonstrated that overexpression of BMI1 or H-RAS alone and in combination markedly altered MCF10A morphology in 2D culture (Datta *et al.*, 2007). We

therefore studied the MCF10A derivative cells grown on Cultrex™, a 3D basement membrane extract culture (Figure 1) to determine if additional phenotypic alterations could be observed. Cells cultured in the context of a 3D basement membrane extract (BME) better recapitulates the in vivo structural scaffolding of the microenvironment than simple 2D culture on plastic. BME culture, therefore, provides a means to better observe how cells may behave in vivo. As expected, parental MCF10A cells formed characteristic round clusters with cells undergoing apoptosis in the central region of the clusters, leading to central lumen formation and polarization of cells around this central lumen, indicative of normal luminal differentiation (Debnath *et al.*, 2002). However, overexpression of BMI1 or H-RAS alone resulted in the formation of disorganized clusters of cells without central lumen formation and loss of polarity, indicating a block in normal luminal differentiation and dysregulated morphogenesis. Co-overexpression of BMI1 and H-RAS in MCF10A cells led to highly disorganized clusters with a spindle-shaped morphology and frequent mitoses, indicating loss of differentiation as well as a highly proliferative phenotype (Figure 1).

BMI1 cooperates with H-RAS to significantly increase cell proliferation and invasion, and inhibit apoptosis in MCF10A cells—Altered expression levels of BMI1 in MCF10A-derived and human breast cancer cells are shown in Figure 2A. Both MCF10A and MCF10A+H-RAS cells exhibited negligible levels of BMI1 expression, whereas BMI1 was highly expressed in both the MCF10A+BMI1 and MCF10A+H-RAS +BMI1 cells. Overexpression of H-RAS alone in MCF10A cells resulted in a statistically significant increase ($p < 0.01$) in proliferation in comparison to parental MCF10A and MCF10A+BMI1 cells at 1 and 3 days in culture (Figure 2*B*, left). After two days, overexpression of BMI1 or H-RAS alone led to a statistically significant increase in proliferation over MCF10A alone ($p < 0.01$), whereas the combination of BMI1 and H-RAS resulted in the highest increase in proliferation at all time points ($p < 0.01$). Conversely, overexpression of BMI1 or H-RAS alone led to a statistically significant decrease in apoptosis in response to etoposide-induced DNA damage compared to parental MCF10A cells, whereas overexpression of both BMI1 and H-RAS resulted in a further statistically significant decrease in apoptosis ($p < 0.01$) at 12hr (Figure 2*C*, left). At 24hr, overexpression of BMI1 alone or in combination with H-RAS resulted in a statistically significant decrease in apoptosis ($p < 0.05$) compared to MCF10A or MCF10+H-RAS cells.

The ability of the cell lines to degrade and migrate through extracellular matrix was measured. While MCF10A cells have negligible (<1%) invasive capability in Matrigel (measured as the number of cells that migrated through the Matrigel barrier), cells overexpressing BMI1 or H-RAS exhibited a 12% and 11% rate of invasion, respectively, compared to parental MCF10A cells, whereas overexpression of both BMI1 and H-RAS resulted in 31% invasion (Figure 2*D*, left). Together, these data show that BMI1 overexpression leads to increased proliferation and invasion, decreased DNA damage-induced apoptosis, and that these effects are greatly augmented through cooperation with H-RAS.

Reduction in BMI1 results in decreased proliferation and increased apoptosis in vitro—Short hairpin RNA (shRNA) for BMI1 was used through transduction with LV-

pLL3.7+BMI1-i to reduce expression of BMI1 in four human breast cancer cell lines that overexpress BMI1: MCF10A-BMI1+H-RAS, MCF-7, MDA-MB-231, and ZR75-1. In each cell line, lentiviral transduction efficiency was >95% as indicated by GFP expression, and BMI1 expression was significantly reduced (Figure 2A). Proliferation of cells with knockdown of BMI1 was significantly decreased ($p < 0.01$) in comparison to cells transduced with empty vector alone (LV-pLL3.7) (Figure 2*B*, right).

Cell lines were treated with 100μM etoposide for 24 hours, after which relative levels of apoptosis were measured. For the MDA-MB-231, ZR75-1, and MCF-7 cell lines, there was a trend towards an increase in the apoptotic response to etoposide in cells transduced with shRNA for BMI1 (Figure 2*C*, right), with a statistically significant increase in apoptosis in the ZR75-1 cell line ($p < 0.05$, Student's T-test), suggesting that the expression of BMI1 in some established breast cancer cell lines confers a resistance to apoptosis induced by DNA damaging agents. In three of four cell lines tested, knockdown of BMI1 led to a significant decrease in invasion ($p < 0.05$, Student's T-test) (Figure 2*D*, right). Western blot analysis revealed that MCF10A-derived cell lines treated with etoposide exhibited attenuated p53 and caspase 3 responses, and decreased levels of XIAP (Figure 3).

BMI1 increases metastatic incidence and leads to metastatic spread to the brain—Although MCF10A and MCF10A+BMI1 cells did not form primary tumours, MCF10A+H-RAS and MCF10A+H-RAS+BMI1 cells produced primary tumours in 100% of xenografted animals. In animals xenografted with MCF10A+H-RAS+BMI1 cells, tumours developed more rapidly over time compared to animals xenografted with MCF10A +H-RAS cells (Figure 4A). Tumours arising from MCF10A+H-RAS+BMI1 cells exhibited significantly more activated (phosphorylated) MAPK (Erk1/2) (Thr202/Tyr204) than MCF10A+H-RAS cells (Figure 4B), consistent with our earlier in vitro studies (Datta *et al.*, 2007). Micro- and macro-metastases were only observed in the livers in 5/10 (50%) and in the spleens of 4/10 (40%) of the mice receiving MCF10A+H-RAS cells, whereas metastasis to both the liver and spleen were observed in 10/10 (100%) of MCF10A+H-RAS+BMI1 xenografted animals (Figure 5). Importantly, spontaneous brain metastasis was found in 3/10 (30%) of the mice receiving MCF10A+H-RAS+BMI1 xenografts (Figure 5), whereas no spontaneous metastases to the brain were found in any of the MCF10A+H-RAS xenograft mice. This demonstrates that collaboration of BMI1 and H-RAS leads to the highly clinically relevant spontaneous development of brain metastasis from these cells.

BMI1 knockdown slows tumour progression in mammary fat pad xenografts

Our results demonstrated that MCF10A+H-RAS+BMI1 cells were highly proliferative and metastatic in fat pad xenografts. Similarly, MDA-MB-231 cells have been well characterized as being tumorigenic and metastatic. Since MCF7 cells do not readily form tumours or metastasize in mice, MCF7 and MCF7 cells with BMI1 knockdown were not used for xenograft studies.

MCF10A+H-RAS+BMI1 cells expressing empty vector (pLL3.7) or shRNA for BMI1 (BMI1-i) were used for mammary fat pad and tail vein injection experiments. Significant but incomplete knockdown of BMI1 (Figure 2A) did not alter the histologic phenotype nor

incidence of primary or metastatic lesions of MCF10A+H-RAS+BMI1 and MDA-MB-231 tumours (data not shown). Tumours arising from cells with BMI1 knockdown were histologically similar to tumours developing from cells without BMI1 knockdown as assessed by H&E staining reviewed by a veterinary pathologist. However, tumour volumes from MCF10A+H-RAS+BMI1 fat pad xenografts with reduced BMI1 expression were significantly decreased compared to cells with higher BMI1 expression (Figure 4*C*) ($p < 0.05$, Two-Way ANOVA with Bonferroni correction). Similarly, there was a significant delay in the onset of primary tumour formation when MDA-MB-231 cells with BMI1 knockdown were injected into fat pads compared to cells with empty vector (Figure 4*D*). 60% of animals at day 49 and 70% of animals at day 56 post-injection of control MDA-MB-231 cells transduced with empty vector developed palpable tumours, whereas only 10% of animals injected with MDA-MB-231 cells transduced with shRNA for BMI1 had tumours at these time points ($p < 0.05$, Two-way ANOVA with Bonferroni correction). Persistent knockdown of BMI1 in these tumours was confirmed by Western blot (Supplementary Figure 1). Taken together, these data demonstrate that decreasing the expression of BMI1 in these breast cancer cells leads to a delay in tumour progression.

BMI1 cooperates with H-RAS resulting in fulminant pulmonary tumours following tail vein injection—Tail vein injections were performed using the MCF10A-derived cell lines. Mice injected with MCF10A+H-RAS+BMI1 cells developed a roughened haircoat, hunched posture, and elevated respiratory rate by 4-5 weeks post-injection. At this time, necropsy revealed fulminant gross metastases involving large portions of all lung lobes of mice injected with MCF10A+H-RAS+BMI1 cells (Figure 6*A*, *right*). In contrast, lungs of mice injected with MCF10A+H-RAS cells were grossly unremarkable at 4-5 weeks (Figure 6*A*, left). At 14-16 weeks post-injection, MCF10A+H-RAS injected mice had histologically small (1-2mm), expansile, non-infiltrative, well-differentiated adenomatous lesions (Figure 6*B*, left). In contrast, after only 4 weeks post-injection, pulmonary metastases in mice injected with MCF10A+H-RAS+BMI1 cells were composed of sheets and bundles of poorly-differentiated spindle-shaped cells with large pleomorphic nuclei demonstrating a high mitotic rate (2-4/hpf), and effacing large portions of the normal pulmonary architecture (Figure 6*B*, right).

BMI1 enhances disseminated tumour cell survival—In order to examine the potential differences in the dynamics of cell survival between GFP-labelled MCF10A+H-RAS and MCF10A+H-RAS+BMI1 cells injected by tail vein, we measured changes in the rates of proliferation, apoptosis and survival of these cells over time in the lungs of mice. Mice were sacrificed at two hours, two days, one week, and four weeks following tail vein injection. Lungs were imaged using an ex-vivo imaging system to detect the presence of GFP-expressing metastatic foci (Figure 6*C, D*). At two hours, the number of MCF10A+H-RAS or MCF10A+H-RAS+BMI1 cells present in the lungs was similar. However, at two days post injection, there was a significant decrease in the number of cells in the lungs of MCF10A+H-RAS injected mice, indicating massive die-off ($p < 6\times10^{-6}$, Student's T-test) compared to MCF10A+H-RAS+BMI1 injected mice. At one and four weeks following injection, MCF10A+H-RAS+BMI1 cells continued to proliferate, ultimately culminating in large tumour masses, in contrast to MCF10A+H-RAS injected mice, in which few cells were

detectable. These data suggest that MCF10A cells overexpressing BMI1 and H-RAS persist and continue to proliferate in the pulmonary circulation to form invasive tumours, whereas H-RAS overexpressing cells undergo rapid and massive loss soon after injection.

BMI1 enhances proliferation and suppresses apoptosis of MCF10A+H-RAS metastatic cells

Ki67 and TUNEL staining were evaluated in pulmonary tumours early in the course of disease and at disease endpoints - 5 weeks post-injection for IV xenografts and approximately 60 days post-injection for mammary fat pad xenografts (Figure 7 and Supplementary Figure 2). Early in the course of disease, there was a statistically significant increase in Ki67 labelling at two days ($p < 0.01$) and one week ($p < 8\times10^{-12}$, Student's T-test) in tumour cells within the lung in the MCF10A+H-RAS+BMI1 group as compared to the MCF10A+H-RAS group (Figure 7*A*). A statistically significant decrease in apoptosis was also observed in the tumour cells within the lung ($p < 0.05$, Student's T-test) in the H-RAS+BMI1 group as compared to the H-RAS group as measured by TUNEL staining (Figure 7*B*).

In end-stage tumours, there was significantly greater staining for Ki67 in MCF10A+H-RAS +BMI1 fat pad tumours ($p < 1.3\times10^{-7}$) and intravenously disseminated lung tumours ($p < 0.0002$, Student's T-test) compared to those arising from H-RAS xenografts (Figure 7*C*), indicating that xenografts overexpressing BMI1 and H-RAS have markedly higher proliferative rates than xenografts overexpressing H-RAS alone. In contrast, TUNEL staining was significantly increased ($p < 0.0002$, Student's T-test) in H-RAS fat pad xenografts in comparison to H-RAS+BMI1 xenografts (Figure 7*D*). Interestingly, there was a lack of significant TUNEL staining in the end-stage lung lesions from both cells types following intravenous cell injection. This may reflect selection for clones in which apoptotic mechanisms are suppressed for the H-RAS overexpressing cells, given the length of time necessary for the development of these slowly progressive and non-infiltrative lesions. Cells overexpressing both BMI1 and H-RAS appear to have gained the ability to evade apoptosis very early, given these results, and the rapid and fulminant pulmonary tumour phenotype.

Table 1 summarizes BMI1 levels and the in vitro and in vivo tumour cell properties of the experiments presented.

DISCUSSION

Recent studies have linked BMI1 expression to a poor prognosis profile in multiple types of cancer, associated with decreased time to disease recurrence and increased metastasis (Glinsky *et al.*, 2005), and anoikis resistance (Glinsky, 2006). In this study, we provide functional evidence that BMI1 can alter the tumorigenic and metastatic phenotype of breast cancer cells.

Interestingly, our results indicate that the ability of BMI1 to increase the aggressive nature of breast cancer cells is likely context dependent. While overexpression of BMI1 alone does increase rates of proliferation and invasion and inhibits the apoptotic response to DNA damage, these effects are significantly augmented in the context of H-RAS, which is

overexpressed in up to 20-30% of human breast cancers. These results would suggest that BMI1 leads to additional molecular alterations that have significant effects on the transformed phenotype, possibly through mechanisms involving global reorganization of chromatin.

Since the MCF10A cells are mutant for p16/ARF, the effects induced by BMI1 must be due to alterations involving other pathways. In our previous work, we demonstrated that BMI1 collaborates with H-RAS to transform HMECs through the dysregulation of multiple growth regulatory pathways, including the AKT and MAPK/ERK pathways, and cell cycle mediators CDK4 and cyclin D (Datta *et al.*, 2007). A recently published report also suggests a p16INKa-independent function of BMI1 in promoting Ewing sarcoma (Douglas *et al.*, 2008). Consistent with our previous in vitro studies (Datta *et al*, 2007), we have demonstrated in this study that tumours arising from MCF10A+H-RAS+BMI1 cells in vivo express significantly more activated MAPK than tumours from MCF10A+H-RAS cells.

We have further demonstrated an important role for BMI1 in maintaining tumorigenic properties of several human breast cancer cell lines. Downregulation of BMI1 in several established breast cancer cell lines results in a significant decrease in proliferation, and increased DNA damage-induced apoptosis. All cell lines with BMI1 knockdown exhibited decreased proliferation and a significant decrease in invasive capability, except the ZR75-1 cell line. Parental ZR75-1 cells are slow-growing and non-invasive (Desprez *et al.*, 1998; He *et al.*, 2006). Knockdown of BMI1 in these cells was lethal over a short time, suggesting that BMI1 is critical for their growth in vitro. This invasive capacity induced by BMI1 expression is consistent with its association with metastatic disease in several types of cancer (Glinsky, 2005) including breast cancer (Kim *et al.*, 2004).

We demonstrated that resistance to DNA damage-induced apoptosis by BMI1 is associated with attenuated p21, p53 and caspase 3 response. Although XIAP, a mediator of cellular survival, is slightly downregulated in MCF10A+H-RAS+BMI1 cells treated with etoposide, the balance of anti- and pro-apoptotic mediators is such that these cells remain resistant to the DNA damage induced effects of etoposide.

Our previous work demonstrated that overexpression of BMI1 alone in MCF10A cells is not sufficient to transform HMECs, whereas overexpression of H-RAS alone or in combination with BMI1 leads to primary tumours with a more poorly differentiated, spindle-shaped morphology and more aggressive tumour growth in vivo (Datta *et al.*, 2007). We have now demonstrated that the overexpression of BMI1 has a marked effect on the incidence and target organ dissemination of metastases. Primary xenograft tumours in the mammary fat pads arising from MCF10A cells overexpressing both BMI1 and H-RAS are associated with significantly increased incidence of spontaneous metastasis to the liver and spleen, in comparison to MCF10A cells only overexpressing H-RAS. Importantly, 30% of mice with primary tumours overexpressing both BMI1 and H-RAS developed metastases to the brain, whereas no brain metastases were observed in mice with the H-RAS tumours. Since the brain is a common location for breast cancer metastases (Clayton *et al.*, 2004; Bendell *et al.*, 2003; Tsukada *et al.*, 1983) but has been extremely difficult to model in animal systems, we believe this is an extremely important and unique observation. Consistent with these

observations, we have shown that knockdown of BMI1 expression in MCF10A+H-RAS +BMI1 cells (Datta *et al.*, 2007) or MDA-MB-231 which carry an H-RAS mutation (Campbell *et al.*, 2006; Mukhopadhyay *et al.*, 1999; Price, 1996), resulted in a statistically significant delay in tumour development through fat pad implantation compared to cells caring empty vector.

Overexpression of BMI1 has been associated with increased incidences of metastasis in human gastric cancer (Huang *et al.*, 2007), breast cancer (Feng *et al.*, 2007; Kim *et al.*, 2004), and melanoma (Mihic-Probst *et al.*, 2007), and in accelerating tumour progression in non-Hodgkin B-cell lymphoma (van Kemenade *et al.*, 2001), Ewing sarcoma (Douglas *et al.*, 2008), oral squamous cell (Kang *et al.*, 2007), nasopharyngeal (Song *et al.*, 2006) and infiltrative ductal carcinoma (Kim *et al.*, 2004). These data illustrate the importance of BMI1 in the development of spontaneous metastasis in breast cancer, and suggest that breast cancers overexpressing H-RAS and BMI1 may be more prone to metastasis.

Using tail vein injection as a model for direct haematogenous spread of tumour cells, we showed that poorly differentiated and aggressive lung tumours developed rapidly and early (4-5 weeks) in the MCF10A+H-RAS+BMI1 injected mice, whereas benign appearing lesions did not appear until late in the course of disease (14-18 weeks) in MCF10A+H-RAS injected mice. Aggressive lung tumours arising in MCF10A+H-RAS+BMI1 tail vein injected mice exhibited a markedly different histologic appearance in comparison with liver, spleen, and brain metastases arising from fat pad injection of MCF10A+H-RAS+BMI1 cells. While the mechanisms regulating these phenotypic distinctions are not known, it is possible that differences in the tissue architecture, microenvironments, stromal-epithelial interactions and tensile strengths at the metastatic site are significantly different.

The mechanisms leading to fulminant pulmonary lesions of MCF10A+H-RAS+BMI1 cells following tail vein injection compared to MCF10A+H-RAS cells are due to marked differences in the rates of proliferation and apoptosis between the cells. MCF10A+H-RAS +BMI1 cells proliferate in an exponential manner over the course of the disease, while there is massive early loss of MCF10A+H-RAS cells by two days after injection. In addition, cells overexpressing both BMI1 and H-RAS are highly resistant to anoikis in vitro, exhibiting a 40-fold increase in the rate of proliferation and a two-third reduction in cell death compared to H-RAS overexpressing cells (data not shown).

In conclusion, we show that expression of BMI1 is critical to the oncogenic behaviour of several established breast cancer cell lines in vitro and in vivo, and most importantly, that the collaboration of BMI1 and H-RAS in HMECs leads to a highly aggressive phenotype that includes increased spontaneous metastasis to the liver and spleen, and novel metastasis to the brain. Furthermore, overexpression of H-RAS and BMI1 enables MCF10A cells to survive, transmigrate, and form fulminant pulmonary metastases in a tail vein model through strong induction of cell proliferation and inhibition of apoptosis, suggesting that breast cancers with BMI1 and H-RAS overexpression may be more metastatic and that BMI1 could be a critical molecular target in patients with cancer and metastatic disease.

Supplementary Material

Refer to Web version on PubMed Central for supplementary material.

ACKNOWLEDGEMENTS

We are grateful to Max Wicha for providing the shRNA lentiviral constructs, George Dunn, Asa Dorsey, and Gail McMullen for animal care, Zi-ayo Liu for lentiviral transductions and Suresh Arya for advice on lentiviral preparation, and Aleksandra Michalowski and the NIH Biostatisitics Branch for assistance with statistical analysis. This work was supported in part by the Intramural Program of the NIH, Center for Cancer Research, National Cancer Institute, and by RO1CA 094150 (GD).

REFERENCES

Bendell JC, Domchek SM, Burstein HJ, Harris L, Younger J, Kuter I, et al. Central nervous system metastases in women who receive trastuzumab-based therapy for metastatic breast carcinoma. Cancer. 2003; 97:2972–7. [PubMed: 12784331]

Brackstone M, Townson JL, Chambers AF. Tumour dormancy in breast cancer: an update. Breast Cancer Res. 2007; 9:208. [PubMed: 17561992]

Campbell MJ, Esserman LJ, Zhou Y, Shoemaker M, Lobo M, Borman E, et al. Breast cancer growth prevention by statins. Cancer Res. 2006; 66:8707–14. [PubMed: 16951186]

Clayton AJ, Danson S, Jolly S, Ryder WD, Burt PA, Stewart AL, et al. Incidence of cerebral metastases in patients treated with trastuzumab for metastatic breast cancer. Br J Cancer. 2004; 91:639–43. [PubMed: 15266327]

Datta S, Hoenerhoff MJ, Bommi P, Sainger R, Guo W-J, Dimri M, et al. Bmi-1 Cooperates with H-Ras to Transform Human Mammary Epithelial Cells via Dysregulation of Multiple Growth-Regulatory Pathways. Cancer Research. 2007; 67:10286–10295. [PubMed: 17974970]

Debnath J, Mills KR, Collins NL, Reginato MJ, Muthuswamy SK, Brugge JS. The role of apoptosis in creating and maintaining luminal space within normal and oncogene-expressing mammary acini. Cell. 2002; 111:29–40. [PubMed: 12372298]

Desprez PY, Lin CQ, Thomasset N, Sympson CJ, Bissell MJ, Campisi J. A novel pathway for mammary epithelial cell invasion induced by the helix-loop-helix protein Id-1. Mol Cell Biol. 1998; 18:4577–88. [PubMed: 9671467]

Dimri GP, Martinez JL, Jacobs JJ, Keblusek P, Itahana K, Van Lohuizen M, et al. The Bmi-1 oncogene induces telomerase activity and immortalizes human mammary epithelial cells. Cancer Res. 2002; 62:4736–45. [PubMed: 12183433]

Douglas D, Hsu JH, Hung L, Cooper A, Abdueva D, van Doorninck J, et al. BMI-1 promotes ewing sarcoma tumorigenicity independent of CDKN2A repression. Cancer Res. 2008; 68:6507–15. [PubMed: 18701473]

Feng Y, Song LB, Guo BH, Liao WT, Li MZ, Liu WL, et al. Expression and significance of Bmi-1 in breast cancer. Ai Zheng. 2007; 26:154–7. [PubMed: 17298744]

Fisher B, Jeong JH, Dignam J, Anderson S, Mamounas E, Wickerham DL, et al. Findings from recent National Surgical Adjuvant Breast and Bowel Project adjuvant studies in stage I breast cancer. J Natl Cancer Inst Monogr. 2001:62–6. [PubMed: 11773294]

Glinsky GV. Death-from-cancer signatures and stem cell contribution to metastatic cancer. Cell Cycle. 2005; 4:1171–5. [PubMed: 16082216]

Glinsky GV. Genomic models of metastatic cancer: functional analysis of death-from-cancer signature genes reveals aneuploid, anoikis-resistant, metastasis-enabling phenotype with altered cell cycle control and activated Polycomb Group (PcG) protein chromatin silencing pathway. Cell Cycle. 2006; 5:1208–16. [PubMed: 16760651]

Glinsky GV, Berezovska O, Glinskii AB. Microarray analysis identifies a death-from-cancer signature predicting therapy failure in patients with multiple types of cancer. J Clin Invest. 2005; 115:1503–21. [PubMed: 15931389]

Guo WJ, Zeng MS, Yadav A, Song LB, Guo BH, Band V, et al. Mel-18 acts as a tumor suppressor by repressing Bmi-1 expression and down-regulating Akt activity in breast cancer cells. Cancer Res. 2007; 67:5083–9. [PubMed: 17545584]

Haupt Y, Alexander WS, Barri G, Klinken SP, Adams JM. Novel zinc finger gene implicated as myc collaborator by retrovirally accelerated lymphomagenesis in E mu-myc transgenic mice. Cell. 1991; 65:753–63. [PubMed: 1904009]

Haupt Y, Bath ML, Harris AW, Adams JM. bmi-1 transgene induces lymphomas and collaborates with myc in tumorigenesis. Oncogene. 1993; 8:3161–4. [PubMed: 8414519]

He B, Mirza M, Weber GF. An osteopontin splice variant induces anchorage independence in human breast cancer cells. Oncogene. 2006; 25:2192–202. [PubMed: 16288209]

Huang KH, Liu JH, Li XX, Song LB, Zeng MS. Association of Bmi-1 mRNA expression with differentiation, metastasis and prognosis of gastric carcinoma. Nan Fang Yi Ke Da Xue Xue Bao. 2007; 27:973–5. [PubMed: 17666329]

Jacobs JJ, Scheijen B, Voncken JW, Kieboom K, Berns A, van Lohuizen M. Bmi-1 collaborates with c-Myc in tumorigenesis by inhibiting c-Myc-induced apoptosis via INK4a/ARF. Genes Dev. 1999; 13:2678–90. [PubMed: 10541554]

Kang MK, Kim RH, Kim SJ, Yip FK, Shin KH, Dimri GP, et al. Elevated Bmi-1 expression is associated with dysplastic cell transformation during oral carcinogenesis and is required for cancer cell replication and survival. Br J Cancer. 2007; 96:126–33. [PubMed: 17179983]

Kim JH, Yoon SY, Jeong SH, Kim SY, Moon SK, Joo JH, et al. Overexpression of Bmi-1 oncoprotein correlates with axillary lymph node metastases in invasive ductal breast cancer. Breast. 2004; 13:383–8. [PubMed: 15454193]

Lessard J, Sauvageau G. Bmi-1 determines the proliferative capacity of normal and leukaemic stem cells. Nature. 2003; 423:255–60. [PubMed: 12714970]

Liu S, Dontu G, Mantle ID, Patel S, Ahn NS, Jackson KW, et al. Hedgehog signaling and Bmi-1 regulate self-renewal of normal and malignant human mammary stem cells. Cancer Res. 2006; 66:6063–71. [PubMed: 16778178]

Mihic-Probst D, Kuster A, Kilgus S, Bode-Lesniewska B, Ingold-Heppner B, Leung C, et al. Consistent expression of the stem cell renewal factor BMI-1 in primary and metastatic melanoma. Int J Cancer. 2007; 121:1764–70. [PubMed: 17597110]

Mukhopadhyay R, Theriault RL, Price JE. Increased levels of alpha6 integrins are associated with the metastatic phenotype of human breast cancer cells. Clin Exp Metastasis. 1999; 17:325–32. [PubMed: 10545019]

Price JE. Metastasis from human breast cancer cell lines. Breast Cancer Res Treat. 1996; 39:93–102. [PubMed: 8738609]

Song LB, Zeng MS, Liao WT, Zhang L, Mo HY, Liu WL, et al. Bmi-1 is a novel molecular marker of nasopharyngeal carcinoma progression and immortalizes primary human nasopharyngeal epithelial cells. Cancer Res. 2006; 66:6225–32. [PubMed: 16778197]

Tsukada Y, Fouad A, Pickren JW, Lane WW. Central nervous system metastasis from breast carcinoma. Autopsy study. Cancer. 1983; 52:2349–54. [PubMed: 6640506]

van Kemenade FJ, Raaphorst FM, Blokzijl T, Fieret E, Hamer KM, Satijn DP, et al. Coexpression of BMI-1 and EZH2 polycomb-group proteins is associated with cycling cells and degree of malignancy in B-cell non-Hodgkin lymphoma. Blood. 2001; 97:3896–901. [PubMed: 11389032]

Vernon AE, Bakewell SJ, Chodosh LA. Deciphering the molecular basis of breast cancer metastasis with mouse models. Rev Endocr Metab Disord. 2007; 8:199–213. [PubMed: 17657606]

Wallgren A, Bonetti M, Gelber RD, Goldhirsch A, Castiglione-Gertsch M, Holmberg SB, et al. Risk factors for locoregional recurrence among breast cancer patients: results from International Breast Cancer Study Group Trials I through VII. J Clin Oncol. 2003; 21:1205–13. [PubMed: 12663706]

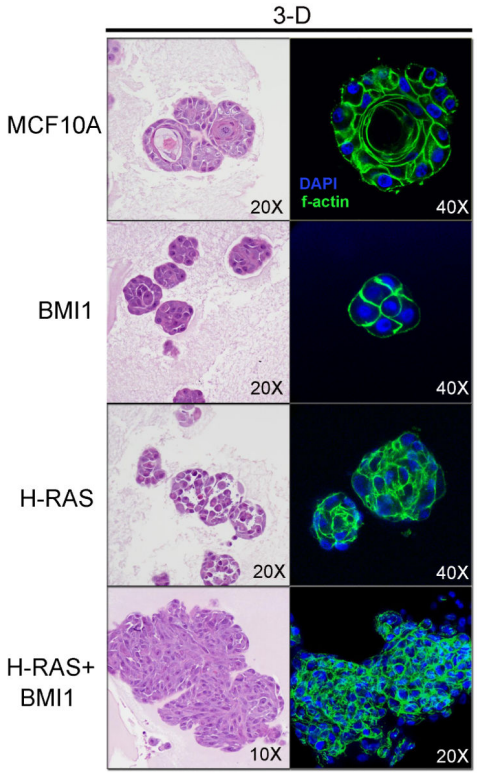

Figure 1.

Morphologic features of MCF10A-derived cell lines cultured in three dimensional Cultrex™. H&E staining (left) and phalloidin staining for f-actin (right). Note characteristic differentiation of MCF10A cells with central lumen formation and polarization of cells. BMI and H-RAS overexpression induce a block in differentiation, and overexpression of both induces disorganized clusters of proliferative, spindle-shaped cells.

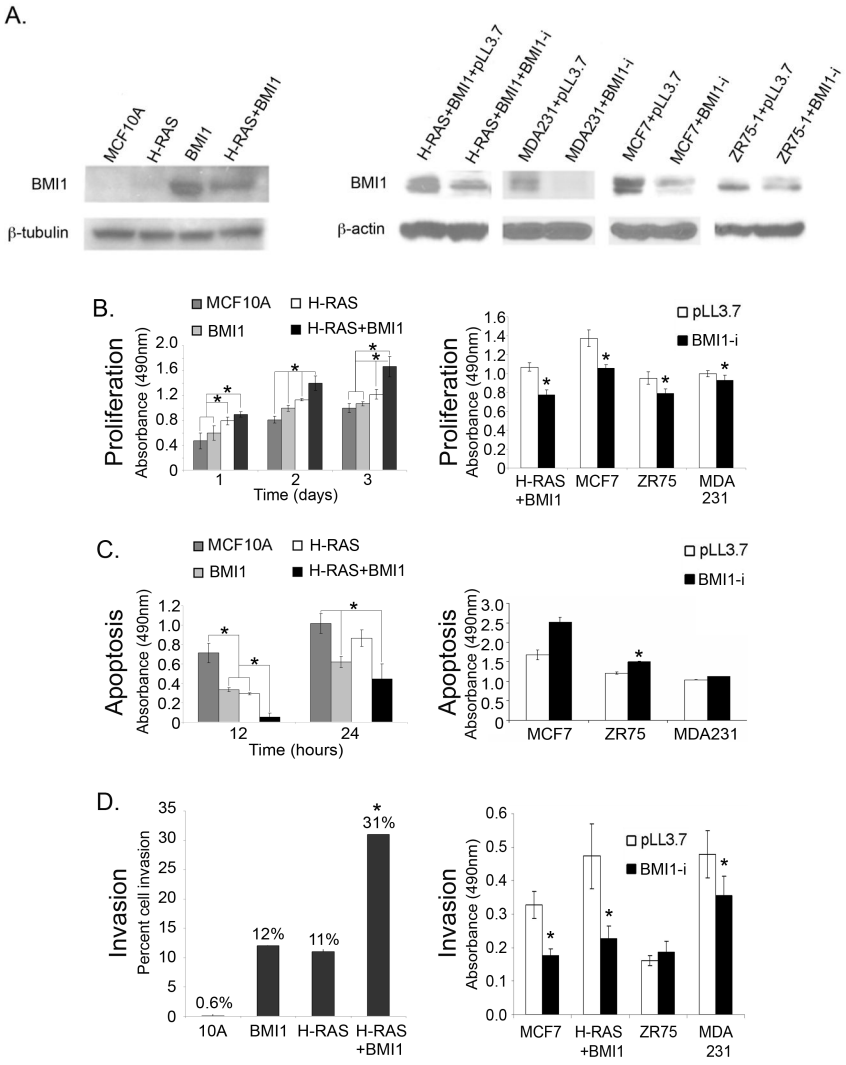

Figure 2. Effects of BMI1 modulation on MCF10A and breast cancer cells

(A) left - BMI1 expression in MCF10A-derived cells: MCF10A; H-RAS - MCF10A+H-RAS; BMI1 - MCF10A+BMI1; H-RAS + BMI1 - MCF10A+H-RAS+BMI1. Right - Reduction in BMI1 expression following stable expression of shRNA in MCF10A +H-RAS + BMI1 cells and MDA-231, MCF7 and ZR75-1 human breast cancer cell lines. (B) Proliferation assays. Left: BMI1 overexpression increases proliferation of MCF10A cells, and in combination with H-RAS further increases proliferation (*$p < 0.01$). Right: Knockdown of BMI1 in breast cancer cell lines decreases proliferation (*$p < 0.01$). MTS-formazan assay. (C) Apoptosis assays. Left: BMI1 overexpression decreases apoptosis of MCF10A cells in response to DNA damage, and in combination with H-RAS further decreases apoptosis (*$p < 0.05$). Right: BMI1 overexpression decreases DNA damage-induced apoptosis in several breast cancer cell lines (*$p < 0.05$). Anti-histone sandwich ELISA. (D) Invasion assays. Left: BMI1 or H-RAS overexpression increase invasion of MCF10A cells, and in combination further increase invasive capability (*$p < 0.05$). Right: Knockdown of BMI1 in several breast cancer cell lines decreases invasion (*$p < 0.05$). Matrigel invasion assay.

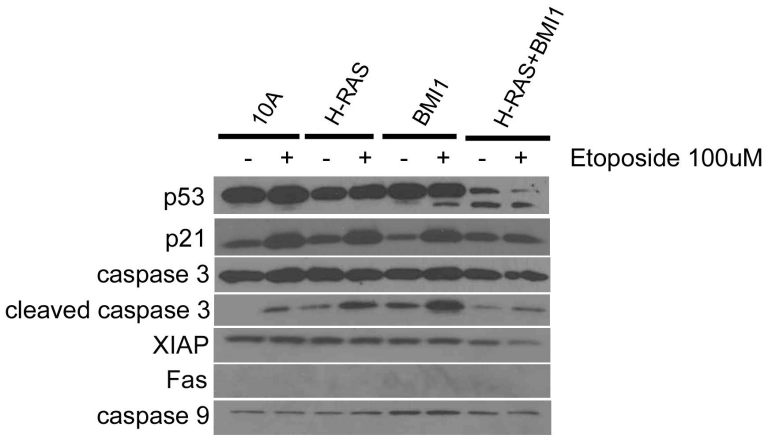

Figure 3. Expression of H-RAS and BMI1 in MCF10A cells reduces expression of genes involved in the apoptotic response to DNA damage

Western blot illustrating blunted expression of p53, p21, and caspase 3 responses in MCF10A+H-RAS+BMI1 cells treated with etoposide.

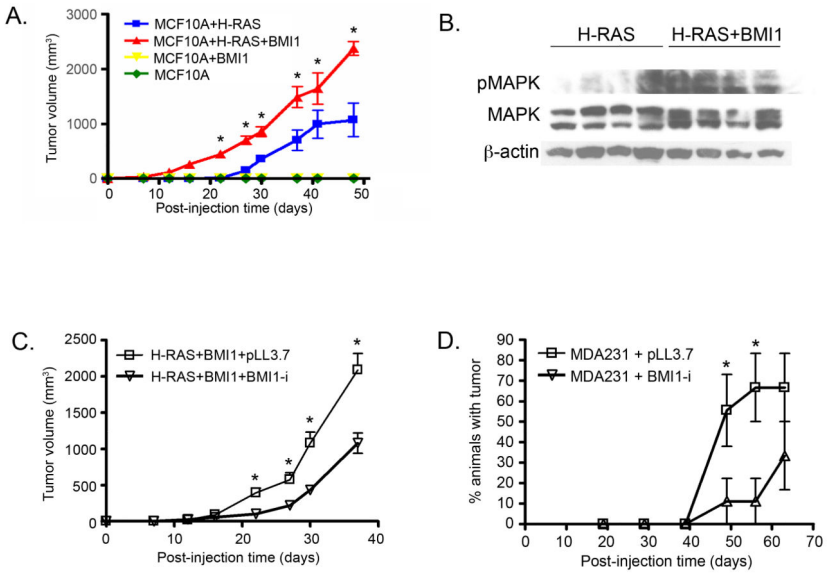

Figure 4. BMI1 expression modulates growth of xenograft tumours

(A) Mammary fat pad xenografts using MCF10A-derived cell lines. BMI1 and H-RAS overexpression together induce larger tumours over time compared to H-RAS alone. (B) Western blot illustrating activation of MAPK pathway in MCF10A cells overexpressing H-RAS and BMI1. (C,D) Mammary fat pad xenografts using MCF10A+H-RAS+BMI1 (C) and MDA-MB-231 (D) cells with BMI1 knockdown (BMI1-i) or empty vector (pLL3.7). BMI1 knockdown delays tumour formation in MCF10A+H-RAS+BMI1 and MDA231 xenografts (*$p < 0.05$).

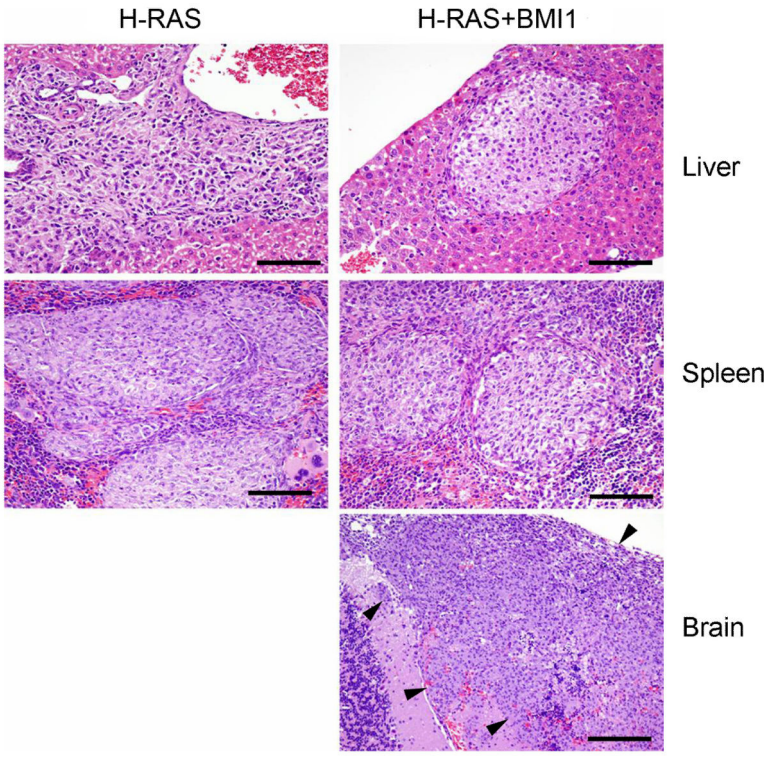

Figure 5. BMI1 augments metastatic progression and induces brain metastasis

Spontaneous metastasis from intra-mammary fat pad MCF10A+H-RAS and MCF10A+H-RAS+BMI1 xenografts. BMI1 overexpression increases metastasis to liver and spleen, and induces novel brain metastasis (Bar = 100 μm).

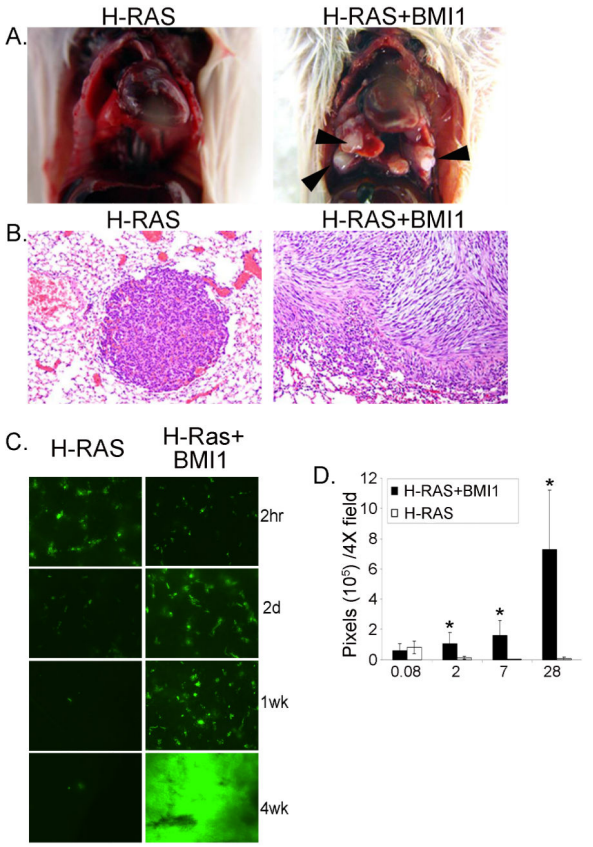

Figure 6. BMI1 in combination with H-RAS induces extensive lung metastases

(A) MCF10A+H-RAS+BMI1 tail vein xenografts show fulminant gross pulmonary metastases involving all lung lobes (right, arrowheads), while other MCF10A-derived tail vein xenografts did not (left). (B) Histologically, mice with MCF10A+H-RAS tail vein xenografts developed small adenomatous lesions late in the disease course (left), while MCF10A+H-RAS+BMI1 xenografts formed destructive lesions (right) that led to rapid clinical illness (Bar = 100 μm). (C) Ex-vivo fluorescent imaging (D) and graphic representation of MCF10A+H-RAS and MCF10A+H-RAS+BMI1 GFP expressing tail vein xenografts. BMI1 overexpression in combination with H-RAS prevents massive loss and induces exponential proliferation of MCF10A cells over time in comparison to H-RAS overexpression alone ($*p < 6\times10^{-6}$, 10 fields observed per time point minimum).

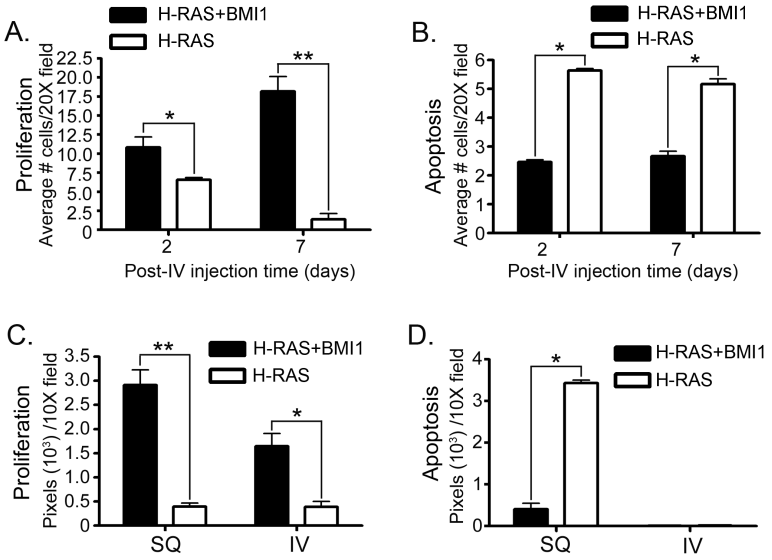

Figure 7. BMI1 overexpression induces severe pulmonary metastasis in combination with H-RAS through increased proliferation and inhibition of apoptosis

Ki67 immunohistochemistry and TUNEL staining in MCF10A+H-RAS (H-RAS) and MCF10A+H-RAS+BMI1 (H-RAS+BMI1) mammary fat pad (SQ) and intravenous (IV) tail vein xenograft models early in disease course (A,B) and at end-stage disease (C,D). There is a significant increase in proliferation (A) at two days (*$p < 0.01$) and one week (**$p < 8\times10^{-12}$) and decrease in apoptosis (B) at two days and one week (*$p < 0.05$) with BMI1 and H-RAS overexpression (10 fields observed minimum). In end stage tumours there is a significant increase in proliferation (C) in SQ (**$p < 1.3\times10^{-7}$) and IV (*$p < 2\times10^{-4}$) xenografts and a significant decrease in apoptosis (D) in SQ xenografts (*$p < 2\times10^{-4}$) with BMI1 and H-RAS overexpression compared to H-RAS alone.

Oncogene. Author manuscript; available in PMC 2010 February 27.

Table 1

Correlation between BMI1 levels, in vitro studies, and in vivo studies

	In vitro			In vivo				
Cell line	***Proliferation***	***Apoptosis***	***Invasion***	***Ki67***	***TUNEL***	***SQ growth*** *	***Metastasis*** Σ	***IV growth*** Ψ
MCF10A	1.0	1.0	1.0	ND	ND	0	0	0
+BMI1	1.3	0.45	20.0	ND	ND	0	0	0
+H-RAS	1.7	0.41	18.3	1.0	1.0	1.0	1(50%) s(60%) b(0%)	1.0
+H-RAS+BMI1	1.9	0.04	51.6	7.3	0.12	2.4	1(100%) s(100%) b(30%)	205.8
+H-RAS+BMI+pLL3.7	1.0	NSD	1.0	ND	ND	1.0	NSD	NSD
+H-RAS+BMI+BMI-li	0.7	NSD	0.5	ND	ND	0.38	NSD	NSD
MDA231+pLL3.7	1.0	1.0	1.0	ND	ND	1.0	NSD	NSD
MDA231+BMI-li	0.9	0.9	0.73	ND	ND	0.16	NSD	NSD
MCF7+pLL3.7	1.0	1.0	1.0	ND	ND	ND	ND	ND
MCF7+BMI-li	0.7	0.7	0.54	ND	ND	ND	ND	ND
ZR75-1+pLL3.7	1.0	1.0	1.0	ND	ND	ND	ND	ND
ZR75-1+BMI-li	0.8	0.8	0.84	ND	ND	ND	ND	ND

Based upon data presented in figures 2-7. Comparisons are made between cell lines in each delineated row; data represents fold change. 0 = no response, ND = not determined, NSD = no significant differences.

*Tumor volume at end of study.

ΨDisseminated lung tumor growth following tail vein injection.

ΣSite/incidence of spontaneous metastasis from mammary fat pad xenografts; 1 = lung, s = spleen, b = brain.